Astrophys Space Sci (2020) 365:42
https://doi.org/10.1007/s10509-020-03754-0

ORIGINAL ARTICLE

Anisotropic compact stars in self-interacting Brans-Dicke gravity

M. Sharif[1] · Amal Majid[1]

Received: 30 December 2019 / Accepted: 20 February 2020 / Published online: 25 February 2020

Abstract This paper focuses on the extension of isotropic spherically symmetric solutions to anisotropic domain by means of minimal geometric deformations in the context of self-interacting Brans-Dicke theory. These deformations decouple the system of field equations into two sets, one describing the isotropic matter field and the other governed by anisotropic source. The former array is evaluated by assuming the metric potentials of isotropic solution (Durgapal-Fuloria/Krori-Barua spacetimes) while additional constraints are applied to solve the later. The junction conditions at the hypersurface of the compact object are employed to determine the unknown constants. The effect of scalar field on physical behavior and viability of all anisotropic solutions is analyzed through regularity and energy conditions. It is observed that anisotropic Krori-Barua solution is viable only for small values of the decoupling parameter whereas the extended Durgapal-Fuloria solution is viable under all constraints.

Keywords Brans-Dicke theory · Gravitational decoupling · Self-gravitating systems

1 Introduction

The study of astrophysical structures (such as stars, galaxies, etc.) contributes significantly to the discovery and comprehension of various relativistic phenomena. In order to explore the intricate nature of self-gravitating systems, analytical solutions of relativistic field equations are required. However, the non-linear differential equations are not only difficult to solve but may yield physically irrelevant solutions as well. Hence, the task of constructing exact as well as viable solutions which adequately describe cosmic objects has attracted the attention of many researchers. Schwarzschild (1916) found the first exact solution of Einstein field equations representing a model with constant density. Since cosmic objects seldom exhibit same density throughout their interior, the quest for improved solutions continued by adopting different techniques.

Ruderman (1972) proposed that anisotropy is a vital property of highly dense systems containing interacting nuclear matter. As observational evidence reveals that nuclear matter exists within stellar structures, anisotropic fluids (with unequal radial (p_r) and tangential (p_t) pressures) are a more suitable representation of cosmic objects as compared to isotropic sources. Existence of pion condensation (Sawyer 1972), phase transition (Sokolov 1980) and super fluid (Kippenhahn and Weigert 1990) are also responsible for introducing anisotropy in an object. The effects of anisotropy on mass, radius, redshift of stars have been explored by considering transverse and radial components of pressure. Herrera and Santos (1997) discussed the causes and effects of anisotropy on massive celestial objects. Harko and Mak (2002) formulated a class of anisotropic solutions by assuming anisotropic factor. According to Mak and Harko (2003), anisotropy is induced in a system due to the presence of a solid core. Hossein et al. (2012) checked viability of anisotropic compact star with a varying cosmological constant.

Ovalle (2008) developed a technique that not only simplifies the extraction of solutions from non-linear field equations but also generates anisotropic solutions. He adopted

✉ M. Sharif
msharif.math@pu.edu.pk

A. Majid
amalmajid89@gmail.com

1 Department of Mathematics, University of the Punjab, Quaid-e-Azam Campus, Lahore, 54590, Pakistan

the method of gravitational decoupling by a minimal geometric deformation (MGD) approach which was originally proposed to deform Schwarzschild metric in the background of Randall-Sundrum brane-world. This approach starts by integrating complex sources, one at a time, with a simple spherical source (also known as seed source) thereby extending the simplest sources to more complex forms. The field equations incorporating the extra source are decoupled by deforming the radial metric component. The decoupled equations consist of two separate sets: one corresponding to the seed source and the other corresponding to the additional source. A complete solution of the whole system is obtained by combining the respective solutions of both sets. Although gravitational decoupling via MGD approach is a breakthrough in the analysis of self-gravitating systems, it is limited to static spherical systems only.

Ovalle and Linares (2013) formulated the counterpart of Tolman IV solution in braneworld by applying MGD approach to the interior of isotropic sphere. This approach was also employed to evaluate new exterior solutions with singular behavior at Schwarzschild radius (Casadio et al. 2015). Ovalle (2017, Ovalle et al. 2018) extended perfect fluid solution to its anisotropic version by decoupling the gravitational sources through MGD approach and examined the behavior of anisotropy and gravitational redshift. Gabbanelli et al. (2018) discussed the physical attributes of anisotropic solutions obtained from isotropic Durgapal-Fuloria (DF) stellar system. Estrada and Tello-Ortiz (2018) obtained well-behaved anisotropic solutions by applying MGD scheme to Heintzmann solution. The MGD approach has also been utilized to extend charged solutions to anisotropic domain. Sharif and Sadiq (2018) investigated the effect of electromagnetic field on viability and stability of anisotropic charged system by considering Krori-Barua (KB) solution as a charged isotropic solution.

The astonishing discovery of an expanding cosmos led astrophysicists to believe in the existence of a hidden anti-gravitational force termed as dark energy. In order to explain the effects and mysterious character of this invisible force, researchers have suggested modifications to general relativity (GR). In 1961, Brans-Dicke (BD) theory (Brans and Dicke 1961), a scalar-tensor generalization of GR, was presented by including a dynamical gravitational constant. Consistent with Mach principle, BD theory effectively reasons the expansion of the universe through a massless scalar field $\varphi = \frac{1}{G(t)}$ which includes the effects of varying gravitational constant. The scalar field is coupled to matter via a coupling parameter ω_{BD} which can be adjusted to get the required results. Larger values of ω_{BD} minimize the modification introduced by the scalar field. Consequently, inflationary era is explained for lower values of ω_{BD} (Weinberg 1989) whereas BD theory complies with weak field tests for $\omega_{BD} > 40{,}000$ (Will 2001). The restrictions on the value of ω_{BD} are removed by incorporating a massive scalar field Φ as well as a potential function $V(\Phi)$ resulting in self-interacting BD (SBD) theory (Khoury and Weltman 2004). In the context of SBD gravity, all values of ω_{BD} greater than $-3/2$ are admissible.

Brans and Dicke (1961) presented the first solution of the BD field equations for a static sphere about a point mass. Sneddon and McIntosh (1974) employed the method given by Geroch (1971) to generate new vacuum BD solutions from vacuum solutions of GR and evaluated the BD solution consistent with NUT solution. Bruckman and Kazes (1977) constructed an exact solution for a perfect fluid model by assuming a linear equation of state. Goswami (1978) converted the BD field equations to Einstein like field equations to derive static as well as non-static solutions. Riazi and Askari (1993) obtained approximate solutions representing static spherical symmetry for the Brans-Dicke field equations in vacuum. Sharif and Manzoor (2015) studied the dynamics of self-gravitating fluids in BD theory with non-zero potential and concluded that models for regular distribution of scalar field are consistent with GR.

Recently, viability and stability of anisotropic solutions, obtained via MGD approach, have also been explored in modified theories (Sharif and Saba 2018; Sharif and Waseem 2019a, 2019b). In this paper, we derive anisotropic solutions for a static sphere by extending known isotropic solutions through gravitational decoupling in SBD theory. The paper is organized as follows. In Sect. 2, we construct field equations with an extra source describing the anisotropic matter distribution. Section 3 gives an overview of the gravitationally decoupled equations obtained via MGD approach. The anisotropic solutions are calculated and checked for viability by imposing two constraints in Sect. 4. In the last section, we summarize our results.

2 Self-interacting Brans-Dicke theory and matter variables

The action of BD theory with a self-interacting potential (Brans and Dicke 1961) in relativistic units ($8\pi G_0 = 1$) is given by

$$S = \int \sqrt{-g}\left(R\Phi - \frac{\omega_{BD}}{\Phi}\nabla^{\gamma}\nabla_{\gamma}\Phi - V(\Phi) + L_m + \beta L_{\Theta}\right) d^4x, \tag{1}$$

where g, R, L_m and L_{Θ} represent determinant of the metric tensor, Ricci scalar, matter Lagrangian and Lagrangian density of a new source, respectively. The new source ($\Theta_{\gamma\delta}$) incorporates physical features of an additional field (scalar, vector or tensor) which introduces anisotropy in the self-gravitating system and can be interpreted as a component of the effective energy-momentum tensor. Variation of the above action with respect to metric tensor and scalar field yields the SBD field equations and evolution equation, respectively, given as

$$G_{\gamma\delta}=T^{(\mathrm{eff})}_{\gamma\delta}=\frac{1}{\Phi}\left(T^{(m)}_{\gamma\delta}+\beta\Theta_{\gamma\delta}+T^{\Phi}_{\gamma\delta}\right), \quad (2)$$

$$\Box\Phi=\frac{\tilde{T}}{3+2\omega_{BD}}+\frac{1}{3+2\omega_{BD}}\left(\Phi\frac{dV(\Phi)}{d\Phi}-2V(\Phi)\right). \quad (3)$$

Here the matter distribution of a perfect fluid in terms of energy density (ρ), pressure (p) and four velocity (u_γ) is represented by the energy-momentum tensor $T^{(m)}_{\gamma\delta}$ as

$$T^{(m)}_{\gamma\delta}=(\rho+p)u_\gamma u_\delta-pg_{\gamma\delta}. \quad (4)$$

Moreover, $\tilde{T}=T^{(m)}+\Theta$, ($T^{(m)}=g^{\gamma\delta}T^{(m)}_{\gamma\delta}$, $\Theta=g^{\gamma\delta}\Theta_{\gamma\delta}$), β is the decoupling parameter and $T^{\Phi}_{\gamma\delta}$ expresses the modified terms arising due to scalar field in the following form

$$T^{\Phi}_{\gamma\delta}=\Phi_{,\gamma;\delta}-g_{\gamma\delta}\Box\Phi+\frac{\omega_{BD}}{\Phi}\left(\Phi_{,\gamma}\Phi_{,\delta}-\frac{g_{\gamma\delta}\Phi_{,\alpha}\Phi^{,\alpha}}{2}\right)$$
$$-\frac{V(\Phi)g_{\gamma\delta}}{2}, \quad (5)$$

where $\Box\Phi=\Phi^{,\gamma}_{;\gamma}=(-g)^{-\frac{1}{2}}[(-g)^{\frac{1}{2}}\Phi^{,\gamma}]_{,\gamma}$.

We discuss the internal distribution of the celestial object by considering the line element describing a static sphere defined by

$$ds^2=e^{\nu(r)}dt^2-e^{\lambda(r)}dr^2-r^2\left(d\theta^2+\sin^2\theta d\phi^2\right). \quad (6)$$

Using Eqs. (2)–(6), the field equations involving the extra source are obtained as

$$\frac{1}{r^2}-e^{-\lambda}\left(\frac{1}{r^2}-\frac{\lambda'}{r}\right)=\frac{1}{\Phi}\left(\tilde{\rho}+T^{0\Phi}_{0}\right), \quad (7)$$

$$-\frac{1}{r^2}+e^{-\lambda}\left(\frac{1}{r^2}+\frac{\nu'}{r}\right)=\frac{1}{\Phi}\left(\tilde{p}_r-T^{1\Phi}_{1}\right), \quad (8)$$

$$\frac{e^{-\lambda}}{4}\left(2\nu''+\nu'^2-\lambda'\nu'+2\frac{\nu'-\lambda'}{r}\right)=\frac{1}{\Phi}\left(\tilde{p}_\perp-T^{2\Phi}_{2}\right), \quad (9)$$

where

$$\tilde{\rho}=\rho+\beta\Theta^0_0,\qquad \tilde{p}_r=p-\beta\Theta^1_1,\qquad \tilde{p}_\perp=p-\beta\Theta^2_2,$$

and

$$T^{0\Phi}_{0}=e^{-\lambda}\left[\Phi''+\left(\frac{2}{r}-\frac{\lambda'}{2}\right)\Phi'+\frac{\omega_{BD}}{2\Phi}\Phi'^2-e^{\lambda}\frac{V(\Phi)}{2}\right],$$

$$T^{1\Phi}_{1}=e^{-\lambda}\left[\left(\frac{2}{r}+\frac{\nu'}{2}\right)\Phi'-\frac{\omega_{BD}}{2\Phi}\Phi'^2-e^{\lambda}\frac{V(\Phi)}{2})\right],$$

$$T^{2\Phi}_{2}=e^{-\lambda}\left[\Phi''+\left(\frac{1}{r}-\frac{\lambda'}{2}+\frac{\nu'}{2}\right)\Phi'\right.$$
$$\left.+\frac{\omega_{BD}}{2\Phi}\Phi'^2-e^{\lambda}\frac{V(\Phi)}{2}\right].$$

The wave equation (3) for the considered scenario is expressed as

$$\Box\Phi=-e^{-\lambda}\left[\left(\frac{2}{r}-\frac{\lambda'}{2}+\frac{\nu'}{2}\right)\Phi'+\Phi''\right] \quad (10)$$

$$=\frac{1}{3+2\omega_{BD}}\left[\tilde{T}+\left(\Phi\frac{dV(\Phi)}{d\Phi}-2V(\Phi)\right)\right], \quad (11)$$

where differentiation with respect to the radial coordinate (r) is denoted by prime. The role of the source $\Theta_{\gamma\delta}$ as a generator of anisotropy can be clearly observed from Eqs. (7)–(9) for $\Theta^1_1\neq\Theta^2_2$. The anisotropy is defined as $\Delta=T^{2(\mathrm{eff})}_{2}-T^{1(\mathrm{eff})}_{1}$. For the present study, we take $V(\Phi)=\frac{1}{2}m^2_{\Phi}\Phi^2$ with m_Φ being the mass of the scalar field.

3 Gravitational decoupling via MGD approach

The field equations (7)–(9) contain eight unknowns (ν, λ, ρ, p, Θ^0_0, Θ^1_1, Θ^2_2, Φ) leading to an underdetermined system of non-linear differential equations. In order to determine the unknowns, we apply gravitational decoupling using the MGD technique proposed by Ovalle (2008). This scheme highlights the influence of source $\Theta_{\gamma\delta}$ on the isotropic model by geometrically deforming the metric potentials ($\nu(r)$ and $\lambda(r)$) through the linear mapping

$$e^{\nu(r)}\mapsto e^{\nu(r)}+\beta h(r), \quad (12)$$

$$e^{-\lambda(r)}\mapsto \xi(r)+\beta f(r), \quad (13)$$

where $h(r)$ and $f(r)$ are the deformations induced in temporal and radial metric functions, respectively. These geometric deformations, being functions of r only, do not disturb spherical symmetry of the solution. The MGD approach complies with the deformation $h\mapsto 0$, i.e., the deformation leaves the temporal component unchanged. Hence, the anisotropic factor is integrated in the radial deformation given in Eq. (13). Employing Eq. (13) in Eqs. (7)–(9) yields two decoupled sets. The first set (corresponding to $\beta=0$) describes the perfect fluid configuration and is given as

$$\rho=-\frac{1}{2r^2\Phi(r)}\left[r^2\omega\xi(r)\Phi'^2(r)-r^2\Phi(r)V(\Phi)\right.$$
$$+r\Phi(r)\left(r\xi'(r)\Phi'(r)2r\xi(r)\Phi''(r)+4\xi(r)\Phi'(r)\right)$$
$$\left.+2\Phi^2(r)\left(r\xi'(r)+\xi(r)-1\right)\right], \quad (14)$$

$$p=\frac{1}{r^2}\left[\Phi(r)\left(r\xi(r)\nu'(r)+\xi(r)-1\right)\right]+\frac{1}{2r\Phi(r)}$$
$$\times\left[\xi(r)\Phi'(r)\left(\Phi(r)\left(r\nu'(r)+4\right)-r\omega_{BD}\Phi'(r)\right)\right]$$

$$-\frac{V(\Phi)}{2}, \tag{15}$$

$$p=\frac{1}{4r\Phi(r)}\big[\Phi(r)\xi'(r)\big(\Phi(r)\big(r\nu'(r)+2\big)+2r\Phi'(r)\big)+\xi(r)\big(2\Phi(r)\Phi'(r)\big(\big(r\nu'(r)+2\big)+2r\Phi''(r)\big)+\Phi^2(r)\big(2r\nu''(r)+r\nu'(r)^2+2\nu'(r)\big)+2r\omega_{BD}\Phi'^2(r)\big)-2r\Phi(r)V(\Phi)\big]. \tag{16}$$

The conservation of energy and momentum for the isotropic system ($\beta=0$) is represented by the equation

$$T_1^{1'(\mathrm{eff})}-\frac{\nu'(r)}{2}\big(T_0^{0(\mathrm{eff})}-T_1^{1(\mathrm{eff})}\big)=0.$$

The effects of source $\Theta_{\gamma\delta}$ are encompassed in the second set expressed as

$$\Theta_0^0=\frac{-1}{2r^2\Phi(r)}\big[r\Phi(r)f'(r)\big(r\Phi'(r)+2\Phi(r)\big)+f(r)\big(r^2\omega_{BD}\Phi'^2(r)+2r\Phi(r)\times\big(r\Phi''(r)+2\Phi'(r)\big)+2\Phi^2(r)\big)\big], \tag{17}$$

$$\Theta_1^1=\frac{-1}{2r^2\Phi(r)}\big[f(r)\big(-r^2\omega_{BD}\Phi'(r)^2+r\Phi(r)\big(r\nu'(r)+4\big)\Phi'(r)+2\Phi^2(r)\big(r\nu'(r)+1\big)\big)\big], \tag{18}$$

$$\Theta_3^3=\frac{-1}{4\Phi(r)}\big[2\Phi(r)\big(rf'(r)\Phi'(r)+f(r)\big(\big(r\nu'(r)+2\big)\Phi'(r)+2r\Phi''(r)\big)\big)+\Phi^2(r)\big(f'(r)\big(r\nu'(r)+2\big)+f(r)\big(2r\nu''(r)+r\nu'^2(r)+2\nu'(r)\big)\big)+2r\omega_{BD}f(r)\Phi'^2(r)\big], \tag{19}$$

with the following conservation equation

$$\Theta_1^{1'(\mathrm{eff})}-\frac{\nu'(r)}{2}\big(\Theta_0^{0(\mathrm{eff})}-\Theta_1^{1(\mathrm{eff})}\big)-\frac{2}{r}\big(\Theta_2^{2(\mathrm{eff})}-\Theta_1^{1(\mathrm{eff})}\big)=0,$$

where

$$\Theta_0^{0(\mathrm{eff})}=\frac{1}{\Phi}\bigg(\Theta_0^0+\frac{1}{2}f'(r)\Phi'(r)+f(r)\Phi''(r)+\frac{\omega_{BD}f(r)\Phi'^2(r)}{2\Phi(r)}+\frac{2f(r)\Phi'(r)}{r}\bigg),$$

$$\Theta_1^{1(\mathrm{eff})}=\frac{1}{\Phi}\bigg(\Theta_1^1+\frac{1}{2}f(r)\nu'(r)\Phi'(r)-\frac{\omega_{BD}f(r)\Phi'^2(r)}{2\Phi(r)}+\frac{2f(r)\Phi'(r)}{r}\bigg),$$

$$\Theta_2^{2(\mathrm{eff})}=\frac{1}{\Phi}\bigg(\Theta_2^2+\frac{1}{2}f'(r)\Phi'(r)+\frac{1}{2}f(r)\nu'(r)\Phi'(r)+f(r)\Phi''(r)+\frac{\omega_{BD}f(r)\Phi'^2(r)}{2\Phi(r)}+\frac{f(r)\Phi'(r)}{r}\bigg).$$

Since both sources (isotropic as well as anisotropic) are individually conserved, no exchange of matter or energy between the two setups is possible. Hence, interactions between the systems are purely gravitational. The MGD approach has converted the system (7)–(9) into a system representing perfect fluid in terms of the variables $\nu(r)$, $\lambda(r)$, ρ, p as well as a simpler set of equations representing anisotropy with four unknowns ($f(r)$, Θ_0^0, Θ_1^1, Θ_2^2). The field equations corresponding to anisotropic interior of the sphere can be solved if an isotropic solution for Eqs. (14)–(16) is known in SBD theory. In order to consider the efficiency of this technique in SBD theory, we consider two isotropic solutions: DF (Durgapal and Fuloria 1985) and KB (Krori and Barua 1975). The physical validity of the anisotropic solutions generated via two ansatz is examined in the next section.

4 Anisotropic solutions

Durgapal and Fuloria obtained a viable perfect fluid solution to describe superdense stellar structures such as neutron stars. The regularity of energy density as well as stability against radial perturbations strengthen the choice of this solution. The singularity-free metric potentials are defined as

$$e^{\nu(r)}=A\big(1+Br^2\big)^4, \tag{20}$$

$$e^{-\lambda(r)}=\xi(r)=\frac{7-B^2r^4-10Br^2}{7(Br^2+1)^2}, \tag{21}$$

where A and B are constants. In the past, anisotropic and charged configurations have been constructed using the above metric functions. To determine the unknown constants, we match the interior and exterior geometries on the hypersurface Σ. The vacuum exterior is described by Schwarzschild line element as

$$ds^2=\bigg(1-\frac{2M}{r}\bigg)dt^2-\frac{1}{(1-\frac{2M}{r})}dr^2-r^2\big(d\theta^2+\sin^2\theta d\phi^2\big), \tag{22}$$

where M is the total mass of the celestial body. The following conditions must be fulfilled at the boundary ($r=R=$ radius of the self-gravitating system) to ensure smooth transition from internal matter distribution to external vacuum

$$\big(g^-_{\gamma\delta}\big)_\Sigma=\big(g^+_{\gamma\delta}\big)_\Sigma,\qquad (p_r)_\Sigma=0,$$
$$\big(\Phi^-(r)\big)_\Sigma=\big(\Phi^+(r)\big)_\Sigma,\qquad \big(\Phi'^-(r)\big)_\Sigma=\big(\Phi'^+(r)\big)_\Sigma.$$

Continuity of the metric components at the hypersurface specifies the constants A and B as

$$A=\frac{R-2M}{R(BR^2+1)^4}, \tag{23}$$

$$B=\frac{-7MR^2-2\sqrt{9R^6-14MR^5}+6R^3}{7MR^4-4R^5}. \tag{24}$$

Krori and Barua presented a static solution for a charged sphere that gained importance due to its singularity-free nature which complies with all the validation tests. The solution was initially limited to charged systems but later researchers analyzed the physical behavior of uncharged systems as well with the help of this solution (Momeni et al. 2015; Zubair and Abbas 2016). Krori-Barua solution is defined by the following metric functions

$$e^{\nu(r)}=e^{Gr^2+H}, \tag{25}$$

$$e^{-\lambda(r)}=\xi(r)=e^{-Fr^2}, \tag{26}$$

where the constants F, G and H are evaluated through the junction conditions $((g^-_{\gamma\delta})_\Sigma=(g^+_{\gamma\delta})_\Sigma)$ as

$$F=\frac{\ln(\frac{R}{R-2M})}{R^2}, \tag{27}$$

$$G=\frac{2M}{R^2(R-2M)}, \tag{28}$$

$$H=\ln\left(1-\frac{2M}{R}\right)-\frac{2M}{R-2M}. \tag{29}$$

Taking the above solutions as seed solutions, we can determine the associated anisotropic interior solutions by considering the respective metric potentials. However, in order to close the system of geometric deformation and source $\Theta_{\gamma\delta}$, certain constraints (a condition on $f(r)$ or an equation of state for $\Theta_{\gamma\delta}$) must be applied. The complete anisotropic solution is characterized by the following state variables

$$\begin{aligned}\rho=\frac{-1}{2r^2\Phi(r)}\big\{&r\Phi(r)\big(r\Phi'(r)\big(\beta f'(r)+\xi'(r)\big)\\&+2\beta f(r)\big(r\Phi''(r)+2\Phi'(r)\big)+\xi(r)\big(r\Phi''(r)\\&+2\Phi'(r)\big)\big)+2\Phi^2(r)\big(\beta rf'(r)-+\beta f(r)+r\xi'(r)\\&+\xi(r)1\big)+r^2\omega_{BD}\Phi'^2(r)\big(\beta f(r)+\xi(r)\big)\\&-r^2\Phi(r)V(\Phi)\big\},\end{aligned} \tag{30}$$

$$\begin{aligned}p_r=\frac{1}{2r^2\Phi(r)}\big\{&r^2(-\omega_{BD})\Phi'^2(r)\big(\beta f(r)+\xi(r)\big)\\&+r\Phi(r)\big(r\nu'(r)+4\big)\Phi'(r)\\&\times\big(\beta f(r)+\xi(r)\big)+2\Phi^2(r)\big(f(r)\big(\beta+\beta r\nu'(r)\big)\\&+r\xi(r)\nu'(r)+\xi(r)-1\big)-r^2\Phi(r)V(\Phi)\big\},\end{aligned} \tag{31}$$

$$\begin{aligned}p_\perp=\frac{1}{4r\Phi(r)}\big\{&2\Phi(r)\big(r\Phi'(r)\big(\beta f'(r)+\xi'(r)\big)\\&+\beta f(r)\big(\big(r\nu'(r)+2\big)\Phi'(r)+2r\Phi''(r)\big)\\&+\xi(r)\big(\big(r\nu'(r)+2\big)\Phi'(r)+2r\Phi''(r)\big)\big)\\&+\Phi^2(r)\big(\beta f'(r)\\&\times\big(r\nu'(r)+2\big)+\beta f(r)\big(2r\nu''(r)+r\nu'^2(r)\\&+2\nu'(r)\big)+2r\xi(r)\nu''(r)+r\nu'(r)\xi'(r)+r\xi(r)\nu'^2(r)\\&+2\xi(r)\nu'(r)+2\xi'(r)\big)+2r\omega_{BD}\Phi'^2(r)\\&\times\big(\beta f(r)+\xi(r)\big)-2r\Phi(r)V(\Phi)\big\},\end{aligned} \tag{32}$$

with anisotropy defined as

$$\Delta=p_\perp-p_r.$$

The constants A, G and H remain unchanged for the anisotropic solution (as temporal component is unperturbed) whereas the constants B and F are treated as free parameters which can be acquired from Eqs. (24) and (27), respectively. Values of the coupling parameter are obtained through the continuity of second fundamental form $((p_r)_\Sigma=0)$, scalar field and its first derivative $((\Phi^-(r))_\Sigma=(\Phi^+(r))_\Sigma$, $(\Phi'^-(r))_\Sigma=(\Phi'^+(r))_\Sigma)$. Moreover, the wave equation is solved numerically to determine the scalar field by taking $m_\Phi=0.1$ (which is in accordance with the constraints imposed by Gravity Probe B experiment). The viability of a model can now be investigated by substituting the corresponding values of constants, $f(r)$, $\nu(r)$, and $\lambda(r)$ in Eqs. (30)–(32). All numerical results are displayed graphically for three values of β (0, 0.1, 0.9) for the star PSR J1614-2230 ($M=1.97\ M_\odot$ and $R=11.29$ km).

4.1 Constraint I

The first constraint requires the radial pressure Θ^1_1 to coincide with isotropic pressure of the seed solution, i.e.,

$$\Theta^1_1=p, \tag{33}$$

which leads to an interior solution compatible with Schwarzschild exterior. Employing Eqs. (15) and (18) in (33) provides the following expression for metric deformation

$$\begin{aligned}f=\frac{1}{\varsigma}\big[&r^2\omega_{BD}\xi(r)\Phi'^2(r)+r^2\Phi(r)V(\Phi)\\&-r\xi(r)\Phi(r)\big(r\nu'(r)+4\big)\Phi'(r)\\&-2\Phi^2(r)\big(r\xi(r)\nu'(r)+\xi(r)-1\big)\big],\end{aligned} \tag{34}$$

where

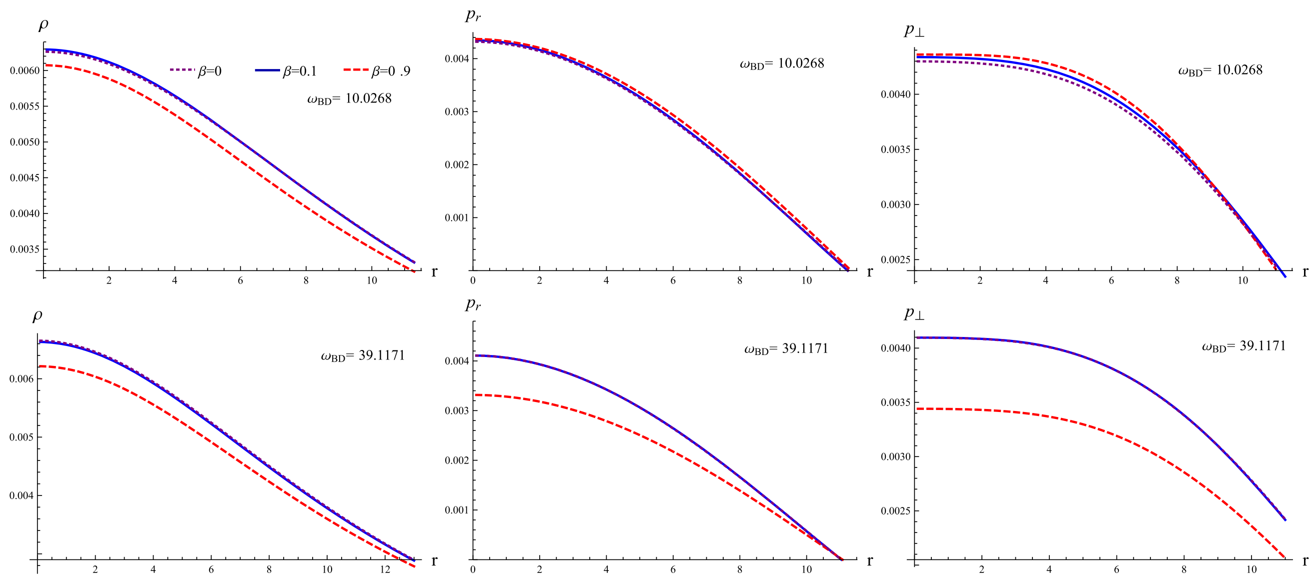

Fig. 1 Plots of ρ, p_r and $p_\perp$ of anisotropic DF solution versus radial coordinate for constraint I

Fig. 2 Anisotropy in extended DF solution for constraint I

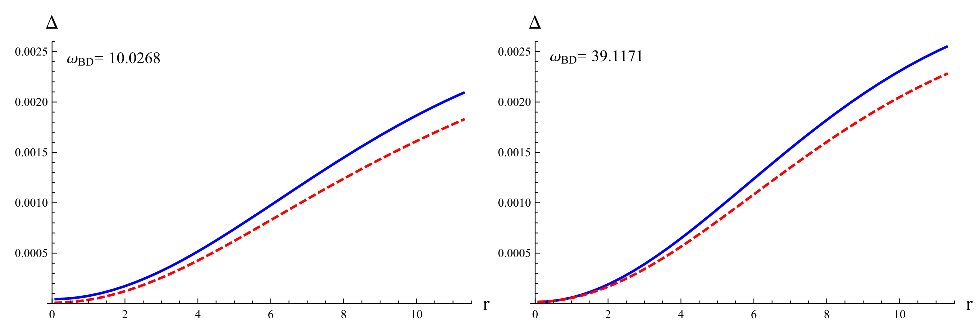

$$\varsigma = r^2\Phi(r)\nu'(r)\Phi'(r) - r^2\omega_{BD}\Phi'^2(r) + 2r\Phi^2(r)\nu'(r) + 4r\Phi(r)\Phi'(r) + 2\Phi^2(r).$$

The junction conditions associated with DF solution yields two values of ω_{BD}: 10.0086 and 39.1171. The plots of density, radial and transverse pressures demonstrate adequate trends (finite throughout and maximum at the center) for both values as shown in Fig. 1. Energy density decreases as β increases in both cases whereas pressure components increase for $\omega_{BD} = 10.0086$ and decrease for $\omega_{BD} = 39.1171$ with an increase in the value of the decoupling parameter. Moreover, positive and increasing anisotropy, portrayed in Fig. 2, suggests the presence of a repulsive anisotropic force counterbalancing the inward force of gravity leading to a stable structure.

It is necessary for the study of compact structures that their interior consists of normal matter, i.e., energy and momentum must be well-defined at every point inside the star. The presence of normal matter is confirmed if four energy conditions (null, weak, strong and dominant) are satisfied. These conditions in the context of SBD gravity are expressed as (Fujii and Maeda 2003)

$$\text{NEC:}\quad \rho + p_r \geq 0, \quad \rho + p_\perp \geq 0,$$
$$\text{WEC:}\quad \rho \geq 0, \quad \rho + p_r \geq 0, \quad \rho + p_\perp \geq 0,$$
$$\text{SEC:}\quad \rho + p_r + 2p_\perp \geq 0,$$
$$\text{DEC:}\quad \rho - p_r \geq 0, \quad \rho - p_\perp \geq 0.$$

Since density and pressure components exhibit positive trend for both values of the coupling parameter, the energy-momentum tensor complies with the first three conditions. The plots for DEC in Fig. 3 display acceptable behavior ensuring physical viability of the anisotropic sphere. The effective mass of the sphere is calculated as

$$M(r) = \frac{R}{2}\left(1 - e^{-\lambda}\right). \tag{35}$$

The ratio of mass to radius of a star gives a measure of its compactness ($u(r)$) which must obey Buchdahl's limit, i.e., $u(r) = \frac{M}{R} < \frac{4}{9}$ (Buchdahl 1959). Buchdahl's limit further

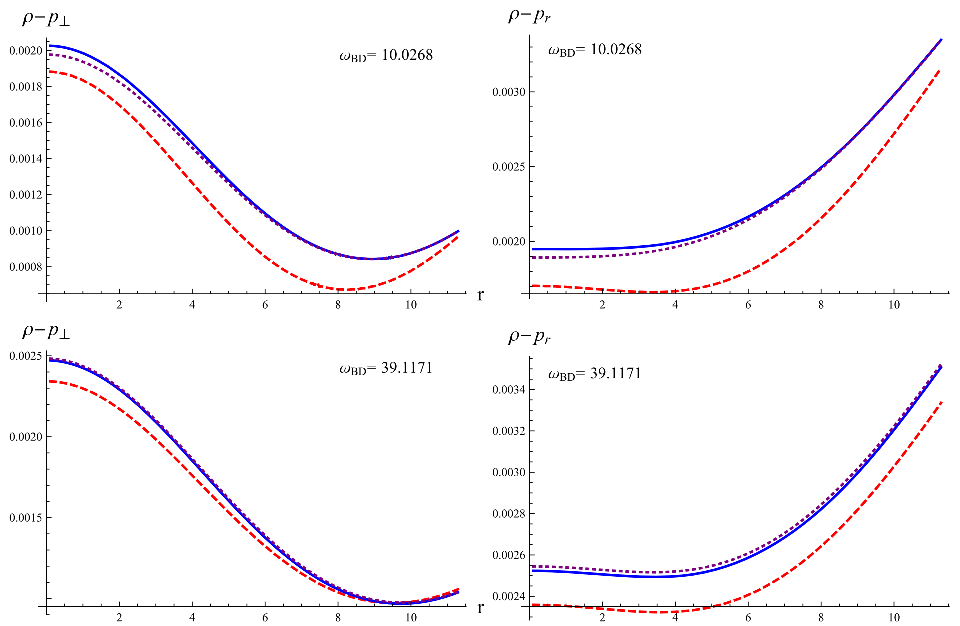

Fig. 3 DEC for anisotropic DF solution with respect to constraint I

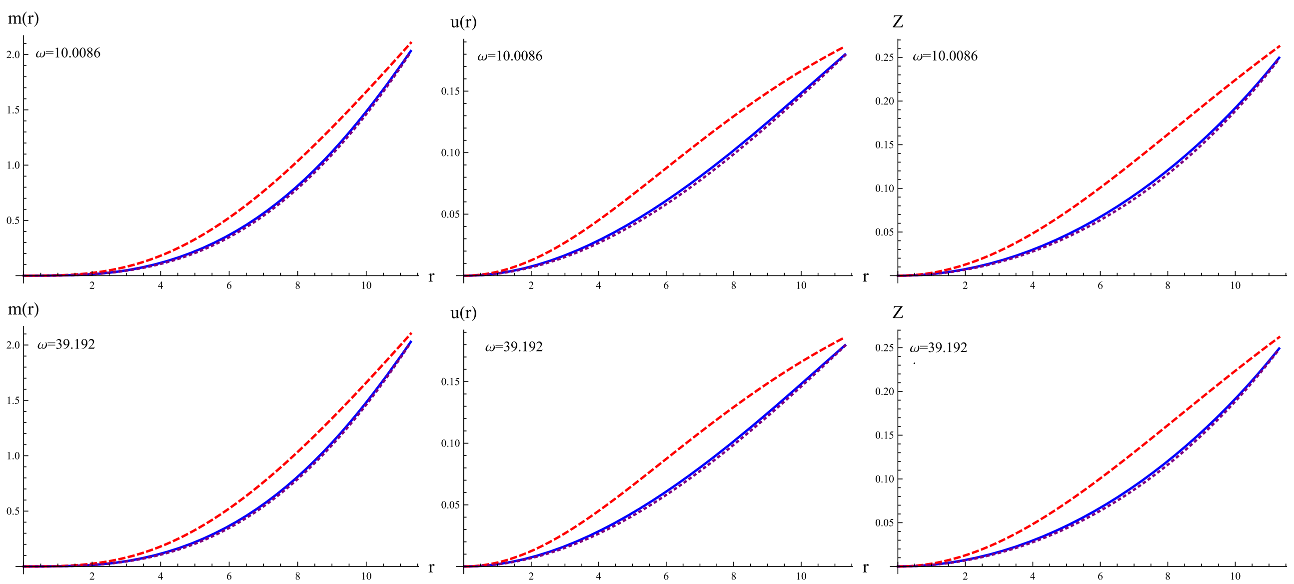

Fig. 4 Plots of m, u and Z corresponding to anisotropic DF solution for constraint I

implies that value of surface redshift ($Z(r) = \frac{1}{\sqrt{1-2u}} - 1$) must not exceed 2 for perfect fluids. However, if the distribution is anisotropic then this limit changes to $Z(r) < 5.211$ (Ivanov 2002). The compactness factor and redshift, plotted in Fig. 4, fulfil the above mentioned requirements.

In the case of anisotropic extension of KB solution, the values of ω_{BD} obtained are 15.831 and 33.7343. The graphical representations of energy density and pressure (radial as well as transverse) in Fig. 5 depict a directly proportional relation between the physical quantities and β. The behavior of anisotropy is analyzed graphically in Fig. 6. For $\beta = 0$, 0.1, the anisotropy is positive whereas anisotropy is initially negative corresponding to $\beta = 0.9$. According to Hossein et al. (2012), the negative anisotropy helps in the formation of a massive star. Hence, the anisotropic model gains stability after a certain distance for $\beta = 0.9$. The physical validity of the solution is checked in Fig. 7 which shows stable configuration for both values of the coupling parameter corresponding to $\beta = 0, 0.1$ while DEC is violated for $\beta = 0.9$. The effective mass, compactness factor and redshift parameter fall within the desired values (Buchdahl 1959; Ivanov 2002) as shown in Fig. 8.

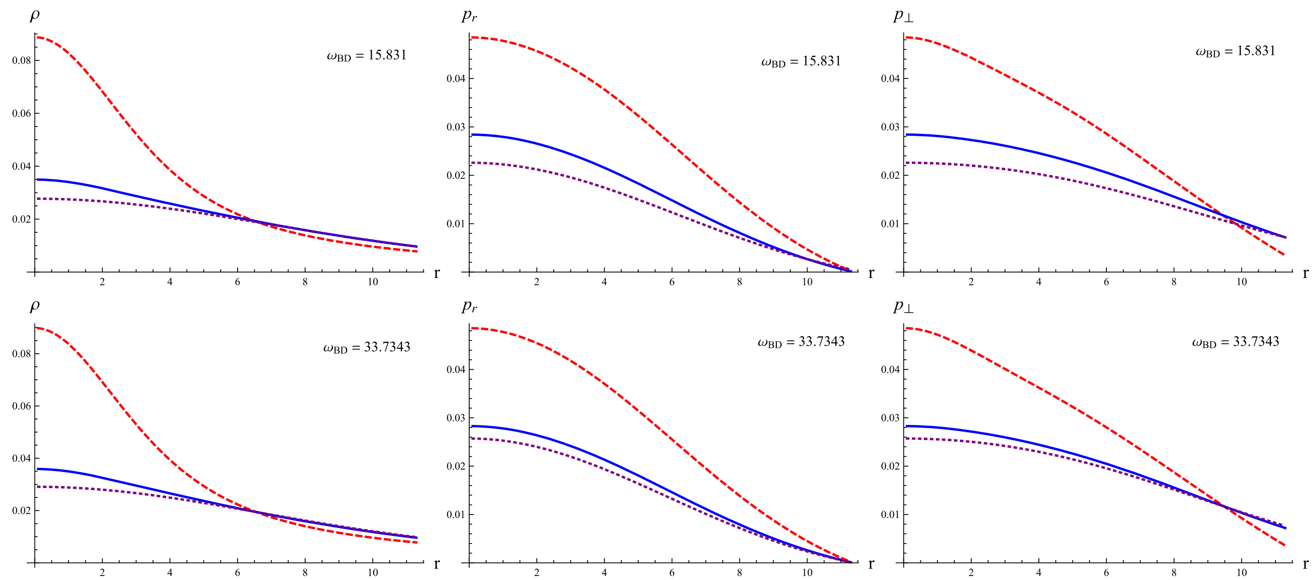

Fig. 5 Plots of ρ, p_r and $p_\perp$ of extended KB solution for constraint I

Fig. 6 Anisotropy in extended KB solution for constraint I

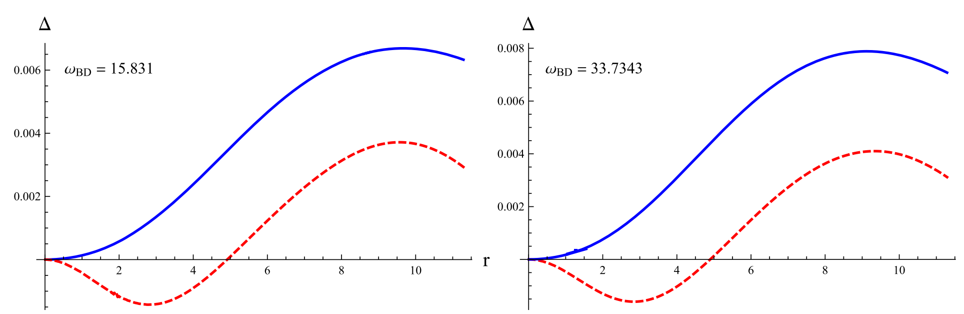

Fig. 7 DEC for extended KB solution with respect to constraint I

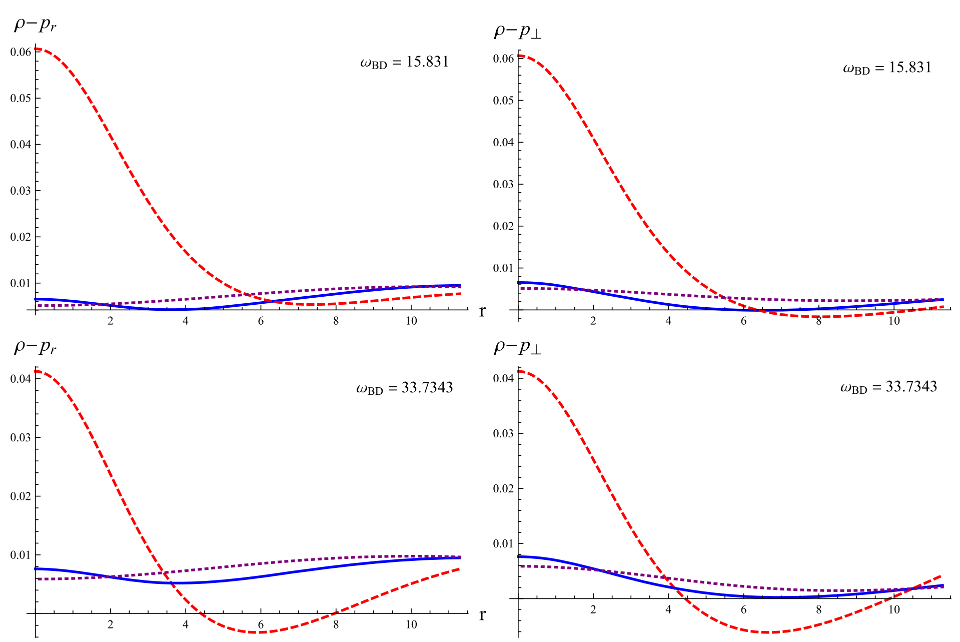

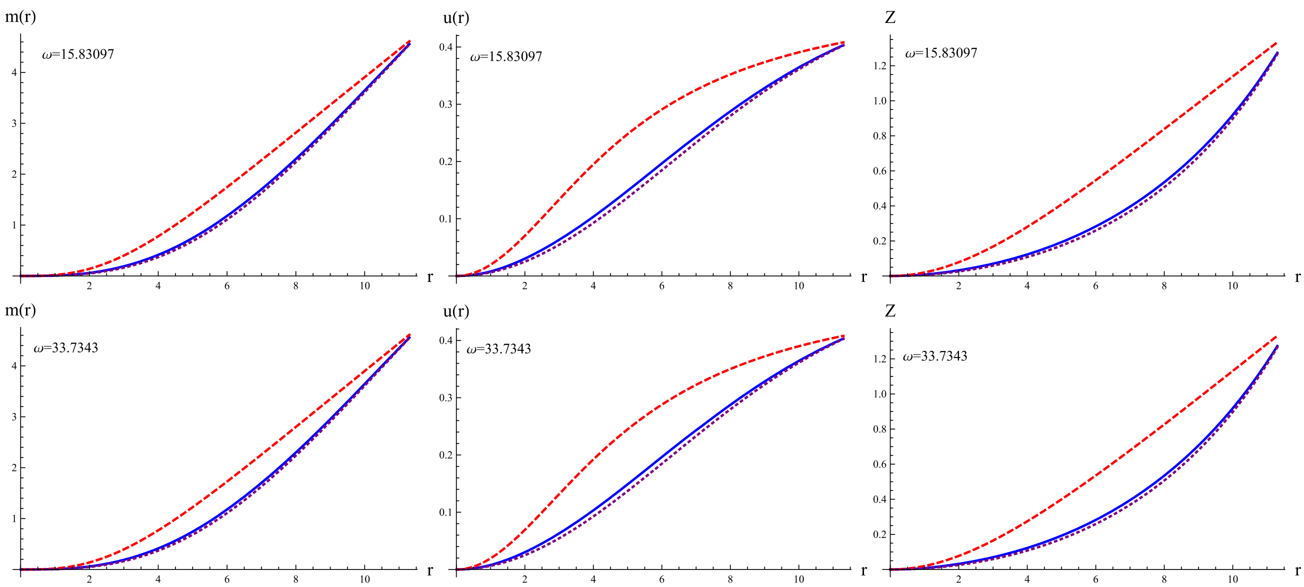

Fig. 8 Plots of m, u and Z corresponding to extended KB solution for constraint I

Fig. 9 Plots of ρ, p_r, $p_\perp$ and Δ of anisotropic DF solution for constraint II

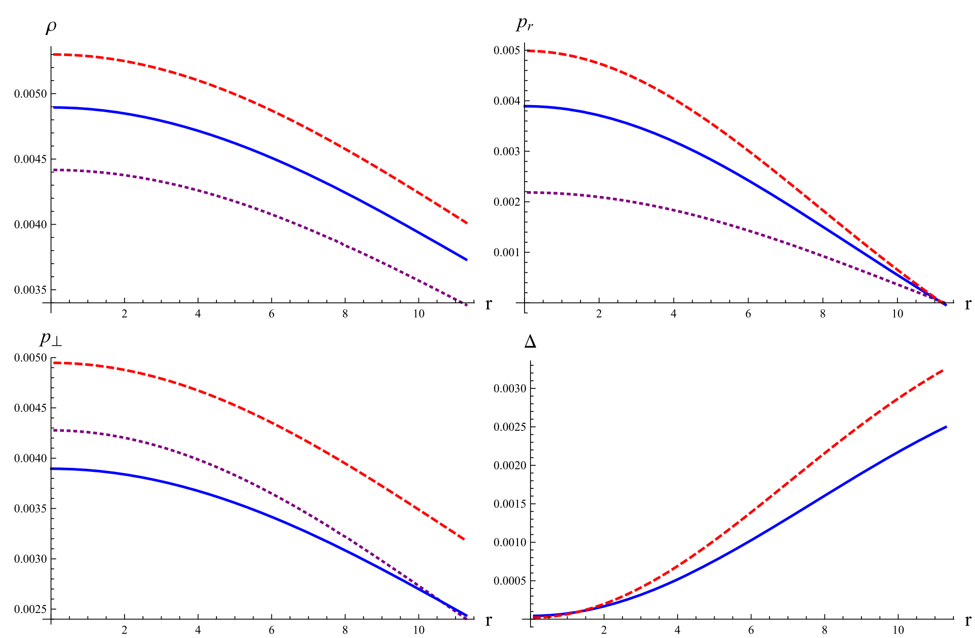

4.2 Constraint II

Another constraint that closes the anisotropic system is

$$\Theta_0^0 = \rho. \tag{36}$$

The differential equation obtained by inserting Eqs. (14) and (17) in the above equation cannot be solved analytically. Hence, by considering the constants computed for DF solution (or KB solution), the wave equation and Eq. (36) are solved numerically. The trend of physical parameters associated with anisotropic version of DF solution is examined graphically in Figs. 9, 10 and 11 for $\omega = 9.89984$. The energy density and pressure components are positive and decrease towards the boundary of the star. Moreover, the positive anisotropy provides a repulsive force. The self-gravitating system is viable as it is consistent with all energy conditions and limits imposed on compactness and surface redshift.

Figures 12, 13 and 14 graphically interpret the state parameters of anisotropic KB solution for $\omega = 14.367$. The model is regular and viable for $\beta = 0$, 0.1 but violates the energy conditions corresponding to a higher value of the decoupling parameter. Further, the surface redshift exceeds the

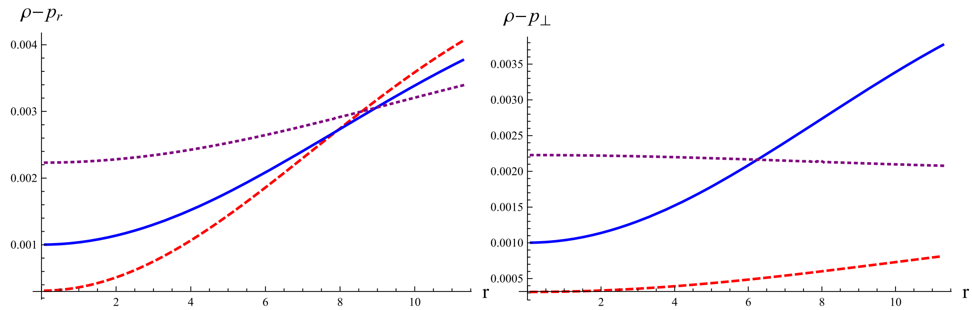

Fig. 10 DEC for anisotropic DF solution with respect to constraint II

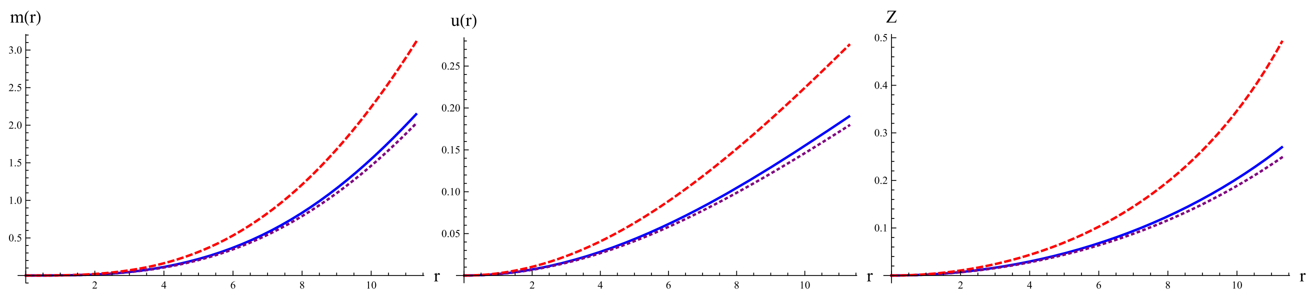

Fig. 11 Plots of m, u and Z corresponding to anisotropic DF solution for constraint II

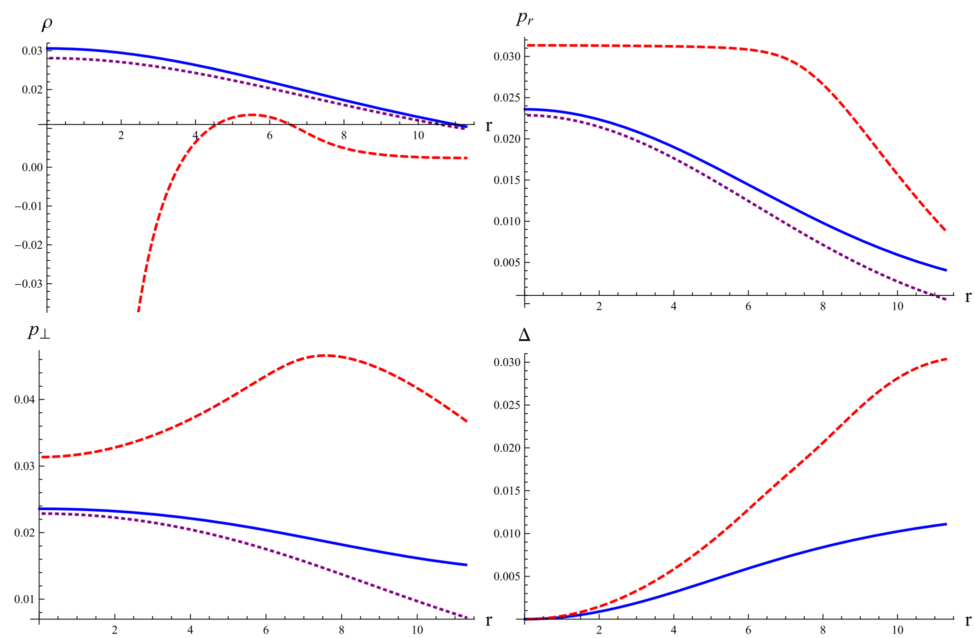

Fig. 12 Plots of ρ, p_r, $p_\perp$ and Δ of extended KB solution for constraint II

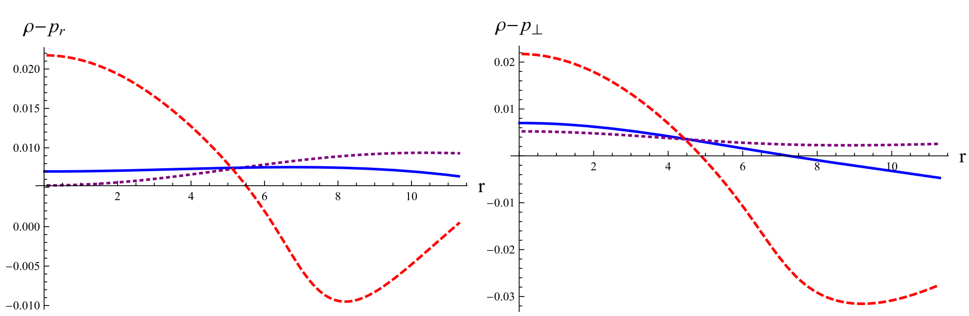

Fig. 13 DEC for extended KB solution with respect to constraint II

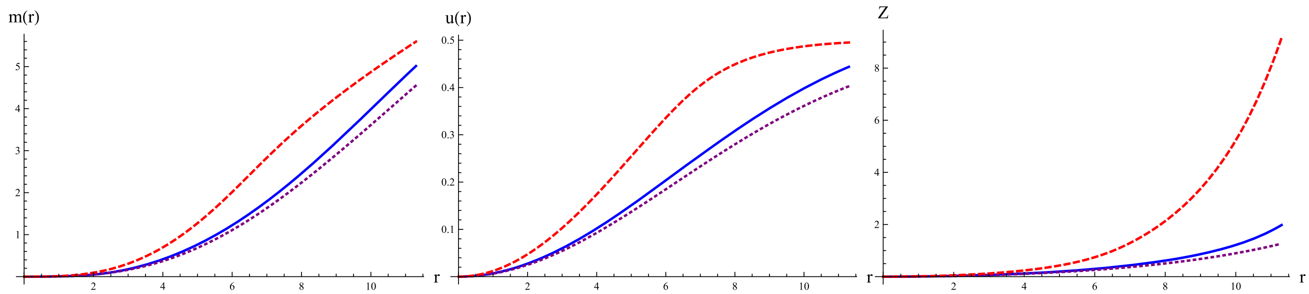

Fig. 14 Plots of m, u and Z corresponding to extended KB solution for constraint II

required limit (Ivanov 2002). Hence, the distribution does not represent valid self-gravitating systems for higher values of the decoupling parameter.

5 Conclusions

The study of self-gravitating objects provides insight into hidden mechanism of the universe. Consequently, many researchers have undertaken the task of finding interior solutions that adhere to the physical behavior and structure of relativistic objects. The technique of gravitational decoupling has proved beneficial in this regard. Self-interacting BD theory allows a dynamical gravitational constant in terms of a scalar field Φ as well as an effective potential function $V(\Phi)$ that adjusts the values of cosmic inflation with the observational data.

In this work, we have employed MGD method to decouple SBD field equations to obtain extended anisotropic versions of interior isotropic solutions. For this purpose, an additional source is introduced in the effective energy-momentum tensor of SBD field equations. After geometric deformation is applied, the system is split into two separate arrays. The isotropic system is specified through metric components of DF as well as KB solutions. Their anisotropic counterparts are evaluated via mimic constraints: $\Theta_1^1 = p$ and $\Theta_0^0 = \rho$. Matching conditions on the boundary of the stellar object determine the unknown constants while the wave equation is utilized to obtain the scalar field. We have also inspected the anisotropic solutions for regularity and viability in the presence of scalar field. Finally, compactness and redshift of self-gravitating system have been analyzed graphically.

Durgapal-Fuloria as well as KB solutions extended via constraint I have maximum energy density at the center which decreases monotonically towards the hypersurface. The anisotropy decreases as β increases implying that the stellar structure is more stable for lower values of the decoupling parameter. For constraint I, the anisotropic DF solution is viable whereas the extended KB solution violates DEC for $\beta = 0.9$. When constraint II is imposed, the anisotropy becomes directly proportional to β indicating increased stability for higher values of the decoupling parameter. The solution linked to DF metric potentials complies with the regularity conditions at the center as well as the energy conditions for all values of β. On the other hand, anisotropic KB solution exhibits negative energy density for $\beta = 0.9$. The dominant energy condition and limit of surface redshift are also breached for this value of the decoupling parameter leading to an unrealistic configuration in case of KB metric potentials. Hence, KB solution yields valid scenarios for small values of the decoupling parameter only. It is interesting to mention here that all the results presented in this paper reduce to GR under the conditions $\Phi =$ constant and $\omega_{BD} \to \infty$.

It is worth mentioning that SBD theory includes the effects of a massive scalar field which increases complexity of non-linear differential equations. Hence the MGD-decoupling represents a useful tool for extending analogue of isotropic solutions for self-gravitating systems in GR into solutions of SBD theory. Moreover, the anisotropic solutions obtained via this technique can be employed to describe various cosmological as well as astrophysical phenomena. It can be utilized, for instance, to investigate the role played by the massive scalar field during gravitational collapse. In the analysis of compact objects, anisotropic solutions containing the effects of scalar field can prove useful in examining the physical characteristics (mass-radius relation, redshift, etc.) of neutron stars, white dwarfs or hypothetical quark stars. We would like to mention here that this approach can be implemented for non-static scenarios as long as the spherical symmetry is preserved under slowly evolving situations.

Acknowledgement This work has been supported by the *Pakistan Academy of Sciences Project*.

References

Brans, C., Dicke, R.H.: Phys. Rev. **124**, 3 (1961)

Bruckman, W.F., Kazes, E.: Phys. Rev. D **16**, 2 (1977)
Buchdahl, H.A.: Phys. Rev. D **116**, 1027 (1959)
Casadio, R., Ovalle, J., da Rocha, R.: Class. Quantum Gravity **32**, 215020 (2015)
Durgapal, M.C., Fuloria, R.S.: Gen. Relativ. Gravit. **17**, 671 (1985)
Estrada, M., Tello-Ortiz, F.: Eur. Phys. J. C **133**, 453 (2018)
Fujii, Y., Maeda, K.: The Scalar-Tensor Theory of Gravitation. Cambridge University Press, Cambridge (2003)
Gabbanelli, L., Rincón, A., Rubio, C.: Eur. Phys. J. C **78**, 370 (2018)
Geroch, R.: J. Math. Phys. **12**, 918 (1971)
Goswami, G.K.: J. Math. Phys. **19**, 442 (1978)
Harko, T., Mak, M.K.: Ann. Phys. **11**, 3 (2002)
Herrera, L., Santos, N.O.: Phys. Rep. **286**, 53 (1997)
Hossein, S.K.M., et al.: Int. J. Mod. Phys. D **21**, 1250088 (2012)
Ivanov, B.V.: Phys. Rev. D **65**, 104011 (2002)
Khoury, J., Weltman, A.: Phys. Rev. D **69**, 044026 (2004)
Kippenhahn, R., Weigert, A.: Stellar Structure and Evolution. Springer, Berlin (1990)
Krori, K.D., Barua, J.: J. Phys. A, Math. Gen. **8**, 508 (1975)
Mak, M.K., Harko, T.: Proc. R. Soc. Lond. Ser. A **459**, 393 (2003)
Momeni, D., et al.: Int. J. Mod. Phys. A **30**, 1550093 (2015)
Ovalle, J.: Mod. Phys. Lett. A **23**, 3247 (2008)
Ovalle, J.: Phys. Rev. D **95**, 104019 (2017)
Ovalle, J., Linares, F.: Phys. Rev. D **88**, 104026 (2013)
Ovalle, J., et al.: Eur. Phys. J. C **78**, 122 (2018)
Riazi, N., Askari, H.R.: Mon. Not. R. Astron. Soc. **261**, 229 (1993)
Ruderman, A.: Annu. Rev. Astron. Astrophys. **10**, 427 (1972)
Sawyer, R.F.: Phys. Rev. Lett. **29**, 382 (1972)
Schwarzschild, K.: Math. Phys. **189** (1916)
Sharif, M., Manzoor, R.: Gen. Relativ. Gravit. **47**, 98 (2015)
Sharif, M., Saba, S.: Eur. Phys. J. C **78**, 921 (2018)
Sharif, M., Sadiq, S.: Eur. Phys. J. C **78**, 410 (2018)
Sharif, M., Waseem, A.: Ann. Phys. **405**, 14 (2019a)
Sharif, M., Waseem, A.: Chin. J. Phys. **60**, 426 (2019b)
Sneddon, G.E., McIntosh, C.B.G.: Aust. J. Phys. **27**, 411 (1974)
Sokolov, A.I.: J. Exp. Theor. Phys. **79**, 1137 (1980)
Weinberg, E.J.: Phys. Rev. D **40**, 3950 (1989)
Will, C.M.: Living Rev. Relativ. **4**, 4 (2001)
Zubair, M., Abbas, G.: Astrophys. Space Sci. **361**, 342 (2016)